A Novel Algorithm Based on the Domain-Decomposition Method for the Full-Wave Analysis of 3-D Electromagnetic Problems

Lei Yin, Jie Wang, and Wei Hong, *Member, IEEE*

***Abstract*—A novel technique based on the domain-decomposition method and frequency-domain finite-difference method is presented for the full-wave analysis of three-dimensional electromagnetic problems. In this method, the original domain is decomposed into sub-domains, Maxwell's equations are then solved in each sub-domain independently, and the global solution is achieved finally by an iterative procedure. It greatly reduces the computational complexity and the memory requirement compared with the conventional finite-difference method and method of moments, etc. To reduce CPU time, some techniques, such as the relaxation iterative algorithm, overlapped domain decomposition, and multimesh resolution are also investigated and adopted to accelerate the algorithm. The validity of this algorithm is verified by numerical examples, including the analysis of a multilayered aperture-coupled patch antenna, the scattering characteristic analysis of conducting pillars, and the S-parameters extraction of the air-bridge discontinuity.**

***Index Terms*—Domain decomposition, FDFD, full-wave analysis.**

I. Introduction

RECENTLY, many investigations were focused on the frequency-dependent characterization and modeling of three-dimensional (3-D) electromagnetic (EM) problems. A lot of numerical methods have been presented in literature by using a mathematical model of both integral and differential equations. Among them, the spectral-domain technique (SDA) [1], the space-domain mixed-potential integral-equation (MPIE) method [2], the finite-element method (FEM) [3], the finite-difference time- domain (FDTD) method [4], and the finite-difference frequency-domain (FDFD) method [5] are some popular methods in the field of computational electromagnetics.

The SDA is very efficient for the analysis of the propagation characteristics of hybrid integrated transmission lines, such as finline, microstrip, coplanar waveguides, etc. The fast Fourier transform (FFT) algorithm additionally enhances the efficiency of SDA. However, the SDA is a highly structure-dependent method. The MPIE is widely used for the fast and accurate analysis of multilayered printed circuit structures including 3-D metallizations. The calculation of Sommerfeld integrals involving the dyadic Green's function in a multilayered substrate is the bottleneck of this method. As a very flexible algorithm, a wide variety of structures can be handled by the FEM, but the mesh generation is a difficult task. Suppression of spurious modes is another challenge with respect to the FEM.

The FDTD and FDFD methods discretize the Maxwell's equations directly, and can be easily applied to solve complex problems. For promoting the computational efficiency of these methods, many works have been focused on the improvement of the absorbing boundary condition, such as the perfectly matched layer (PML) and dispersive boundary condition (DBC) [6], etc. These improvements greatly reduced the computational scale. For electrically large problems, however, these methods will also exhaust all computer resources.

As a promising technique, the domain-decomposition method (DDM) [7], [8] is now widely used in solving large problems. Different from other methods, the DDM decomposes the original large domain into independent small sub-domains. In each sub-domain, the most efficient method can be chosen independently to solve Maxwell's equations defined on it. This will greatly reduce the scale of the original problem. Moreover, it is well suited for numerical implementation on parallel computers, and can considerably reduce both memory requirements and CPU time. The traditional investigations on the DDM in the EM field were focused on the solution of Laplace equations or static problems, e.g., the parameter extraction of 3-D very large scale integration (VLSI) interconnect structures [9], [10]. In recent years, the DDM has been extended to solve Helmholtz equations, such as the two-dimensional (2-D) scattering problem by Strupfel [11] and the Yin *et al.* [12]. However, there are still few reports on the application of DDM–finite-difference (FD) in solving Maxwell's equations.

In this paper, the DDM combined with the FDFD method is presented for the analysis of 3-D EM problems. The iterative algorithm of the DDM is studied, and the implementation of the virtual boundary condition (VBC) introduced in the DDM is also discussed in detail under the FD scheme in Section II. Section III illustrates some typical examples, including the S-parameter extraction of an aperture-coupled stacked microstrip antenna [13], an air-bridge structure, and the scattering analysis of 3-D conducting pillars. To promote the computational efficiency of the method, several accelerating algorithms, such as

Manuscript received March 22, 2000.

L. Yin was with the State Key Laboratory of Millimeter Waves, Department of Radio Engineering, Southeast University, Nanjing 210096, China. He is now with Celestry Inc., San Jose, CA 95134 USA.

J. Wang and W. Hong are with the State Key Laboratory of Millimeter Waves, Department of Radio Engineering, Southeast University, Nanjing 210096, China (e-mail: weihong@seu.edu.cn).

Publisher Item Identifier 10.1109/TMTT.2002.801361.

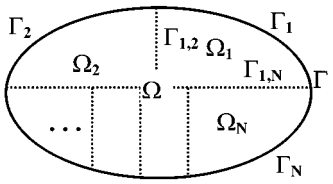

Fig. 1. Model of a 3-D structure.

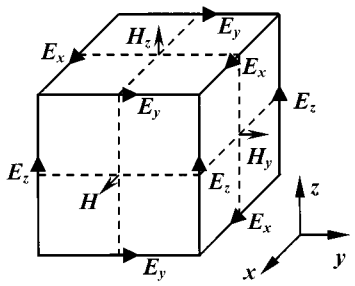

Fig. 2. Yee lattice.

relaxation iterative algorithm, overlapped domain decomposition, and multimesh resolution are also studied in Section IV, and the numerical results demonstrated the accelerating effect compared with the original algorithm.

II. Basic Theory

A. FDFD

Consider an arbitrary 3-D structure, as illustrated in Fig. 1. Let Ω be a boundary open set and $\Gamma = \partial\Omega$ be the boundary of the region Ω. The problem (P) can then be described by following Maxwell's equations

$$(P)\colon \begin{cases} \nabla \times \mathbf{H} = \mathbf{J} + i\omega\varepsilon\mathbf{E} \\ \nabla \times \mathbf{E} = -\mathbf{J}_m - i\omega\mu\mathbf{H}, & \text{in } \Omega \\ \text{Boundary condition}, & \text{on } \Gamma \end{cases}$$

where ω is the frequency and ε and μ are the permittivity and permeability of the medium, respectively. For convenience, rewrite the above equation as follows:

$$(P)\colon \begin{cases} \nabla \times \nabla \times \vec{u} - k^2\vec{u} = \vec{f}, & \text{in } \Omega \\ \nabla \times \vec{u} \times \hat{n} \times \hat{n} + jk\vec{u} \times \hat{n} = \vec{g}, & \text{on } \Gamma \end{cases} \tag{1}$$

where $k = \omega\sqrt{\mu\varepsilon}$ is the wavenumber, $\hat{n}$ is the outward normal vector from Ω, $\vec{u}$ is the electric or magnetic field to be determined, and the functions $\vec{f}$ and $\vec{g}$ indicate the sources. Following the conventional FDFD steps, the structure is discretized by a Yee-type FD lattice, as shown in Fig. 2, and a matrix equation then results by coupling together all the FD equations at the interior nodes and FD-type boundary equations as follows:

$$[S]\overline{\Phi} = \overline{f} \tag{2}$$

where the matrix $[S]$ is a sparse matrix, $\overline{\Phi}$ is the unknown vector that consists of the field components at all nodes, and $\overline{f}$ is a given vector corresponding to the incident fields. After the field components at all nodes are obtained by solving (2), the EM property of the structure can then be easily achieved.

B. Domain Decomposition

Although the coefficient matrix $[S]$ in (2) is a sparse matrix, it might be too huge to be operated. For example, assuming a structure with $length \times width \times height$ as $2\lambda_0 \times 2\lambda_0 \times 1.5\lambda_0$ (λ_0 is the wavelength of free space) and creating 20 grids per λ_0, then a sparse matrix of order 288 000 will result, which will cost nearly 90 MB for only storing it. On the other hand, to accurately model sharp discontinuities, a very small mesh size has to be employed, which will greatly enlarge the scale of the above sparse matrix.

Consider still the model defined in (1), but now divide the region Ω into m arbitrary nonoverlapped sub-domains, which is illustrated in Fig. 1. Let Ω_p, $p = \overline{1, m}$ be one of these sub-domains, $\Gamma_{q,p} = \overline{\Omega}_q \cap \overline{\Omega}_p$ be the interface between two contiguous sub-domains Ω_p and Ω_q, and $\Gamma_p = \overline{\Omega}_p \cap \Gamma$ be the part boundary of Ω_p coinciding with Γ. The original problem defined in (1) is then decomposed into m small problems, which are defined as follows:

$$(P_p)\colon \begin{cases} \nabla \times \nabla \times \vec{u_p} - k^2\vec{u_p} = \vec{f}, & \text{in } \Omega_p \\ \nabla \times \vec{u_p} \times \hat{n}_p \times \hat{n}_p + jk\vec{u_p} \times \hat{n}_p = \vec{g}, & \text{in } \Gamma_p \\ \text{Virtual boundary condition}, & \text{in } \Gamma_{q,p},\ \forall q \neq p \end{cases} \tag{3}$$

where $\hat{n}_p$ is the outward normal from Ω_p. The VBC in this equation is a new condition introduced by additional boundary $\Gamma_{q,p}$. Through it, each sub-domain can exchange information with neighboring sub-domains. The traditional Dirichlet–Numan (D–N) alternating method for solving the Laplace equation only fits for solving static problems, and cannot solve full-wave problems [9], [10]. Desprès solved this problem in [7] by providing a new VBC in iteration type

$$\begin{aligned} &\nabla \times \vec{u}_p^{n+1} \times \hat{n}_p \times \hat{n}_p + jk\vec{u}_p^{n+1} \times \hat{n}_p \\ &\quad = \nabla \times \vec{u}_q^{n} \times \hat{n}_q \times \hat{n}_q - jk\vec{u}_q^{n} \times \hat{n}_q \end{aligned}, \qquad \text{on } \Gamma_{q,p},\ \forall q \neq p. \tag{4}$$

An iterative algorithm based on this condition is then followed:

$$\forall\, n > 0 \text{ and } p = \overline{1, m}$$

and

$$\begin{aligned} &\nabla \times \nabla \times \vec{u}_p^{n+1} - k^2\vec{u}_p^{n+1} = \vec{f}, && \text{in } \Omega_p \\ &\nabla \times \vec{u}_p^{n+1} \times \hat{n}_p \times \hat{n}_p + jk\vec{u}_p^{n+1} \times \hat{n}_p = \vec{g}, && \text{on } \Gamma_p \\ &\nabla \times \vec{u}_p^{n+1} \times \hat{n}_p \times \hat{n}_p + jk\vec{u}_p^{n+1} \times \hat{n}_p \\ &\quad = \nabla \times \vec{u}_q^{n} \times \hat{n}_q \times \hat{n}_q - jk\vec{u}_q^{n} \times \hat{n}_q, && \text{on } \Gamma_{q,p},\ \forall q \neq p \end{aligned} \tag{5}$$

where $\vec{u}_p^{n}$ is the solution in Ω_p at the nth iteration step of the problem (P_p). Although this condition is weakly compared with the D–N condition, it still provides the continuous condition of the fields and its first-order derivatives. On the other hand, it implies the essentiality of wave propagation. Thus, the VBC in (4) ensures the solution on each sub-domain obtained using the above algorithm is the approximate solution of the problem (P). However, the condition shown in (4) cannot be directly employed in the FD scheme. Consider conjoint sub-domains shown in Fig. 3, and still use the Yee-type grid to discretize the

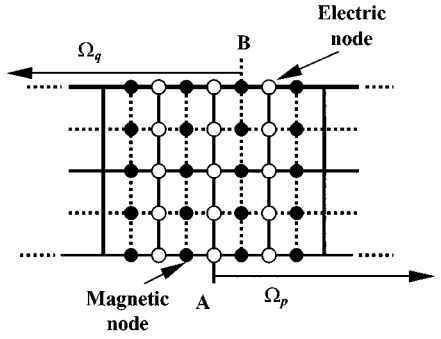

Fig. 3. Virtual boundary under FD equation.

virtual boundary. Equation (4) can then be expressed in the FD equation as

$$\begin{cases} \mu_r H_{y(p)}^{n+1} - j\sqrt{\mu_r\varepsilon_r}E_{x(p)}^{n+1} \\ \quad = \mu_r H_{y(p-1)}^{n} - j\sqrt{\mu_r\varepsilon_r}E_{x(p-1)}^{n} \\ \mu_r H_{x(p)}^{n+1} + j\sqrt{\mu_r\varepsilon_r}E_{y(p)}^{n+1} \\ \quad = \mu_r H_{x(p-1)}^{n} + j\sqrt{\mu_r\varepsilon_r}E_{y(p-1)}^{n} \end{cases}, \qquad \text{on } \Gamma_{p-1,p} \tag{6a}$$

for the left boundary of sub-domain Ω_p and

$$\begin{cases} \mu_r H_{y(p)}^{n+1} + j\sqrt{\mu_r\varepsilon_r}E_{x(p)}^{n+1} \\ \quad = \mu_r H_{y(p+1)}^{n} + j\sqrt{\mu_r\varepsilon_r}E_{x(p+1)}^{n} \\ -\mu_r H_{x(p)}^{n+1} + j\sqrt{\mu_r\varepsilon_r}E_{y(p)}^{n+1} \\ \quad = -\mu_r H_{x(p+1)}^{n} + j\sqrt{\mu_r\varepsilon_r}E_{y(p+1)}^{n} \end{cases}, \qquad \text{on } \Gamma_{p+1,p} \tag{6b}$$

for the right boundary of sub-domain Ω_p. The virtual boundary is located on the plane on which only tangential electrical-field components exist. It is known that the corresponding tangential magnetic-field components on both sides of the virtual boundary are placed a half mesh step beyond or retard this boundary under the Yee-type grid. When employing VBCs (6a) and (6b) directly, the algorithm will be divergence due to the error accumulation in phase. To avoid this problem, one efficient means is to apply one of the VBCs [see (6a) and (6b)] for both of the conjoint sub-domains, which means that the virtual boundary is located on plane A for sub-domain Ω_p and on plane B for sub-domain Ω_q. In this case, the VBCs for conjoint sub-domains employed the same field components and avoided the error accumulation in phase. Based on this improvement, one can easily combine the DDM with FD method to analyze the EM property of complex 3-D structures.

C. Matrix Expression of the Iterative Algorithm

As we know, the FD equations corresponding to each sub-domain can be expressed in a matrix equation as

$$[S_i]\overline{\Phi}_i = \overline{f}_i \tag{7}$$

where $[S_i]$ is the coefficient matrix for the ith sub-domain, $\overline{\Phi}_i$ is the vector for the unknown field components in the ith sub-domain, and $\overline{f}_i$ has resulted from (3) and (4).

Now define $\overline{\Phi}_i^{(k)}$ as the solution of the kth iteration on the ith sub-domain, and $\overline{f}_i^{(k)}$ as the right-hand side of the kth iteration. Since the VBC is the relationship between the solution of the $(k+1)$th iteration on the ith sub-domain and the solution of the kth iteration on the contiguous pth sub-domain, $\overline{f}_i^{(k)}$ can be written as

$$\overline{f}_i^{(k)} = \overline{f}_i^{0} + \sum_{\substack{p=1 \\ p\neq i}}^{m} [V_{p,i}]\overline{\Phi}_p^{(k-1)} \tag{8}$$

where $\overline{f}_i^0$ is the incident field on the ith sub-domain, and $[V_{p,i}]$ is the VBC shown in (4). Hence, the iterative algorithm of (5) can be written in matrix form as

$$\overline{\Phi}^{(k+1)} = \left[\tilde{A}\right]\overline{\Phi}^{(k)} + \mathbf{f}_0 \tag{9}$$

where

$$\overline{\Phi}^{(k)} = \begin{bmatrix} \overline{\Phi}_1^{(k)} \\ \overline{\Phi}_2^{(k)} \\ \vdots \\ \overline{\Phi}_m^{(k)} \end{bmatrix} \tag{10}$$

is the vector of unknowns on all sub-domains for the kth iteration. The matrix

$$\left[\tilde{A}\right] = \begin{bmatrix} 0 & [S_1]^{-1}[V_{2,1}] & \cdots & [S_1]^{-1}[V_{m,1}] \\ [S_2]^{-1}[V_{1,2}] & 0 & \cdots & [S_2]^{-1}[V_{m,2}] \\ \vdots & \vdots & \ddots & \vdots \\ [S_m]^{-1}[V_{1,m}] & [S_m]^{-1}[V_{2,m}] & \cdots & 0 \end{bmatrix} \tag{11}$$

is the so-called Jacobi matrix constructed by block matrices, and

$$\mathbf{f}_0 = \begin{bmatrix} [S_1]^{-1}\overline{f}_1^{0} \\ [S_2]^{-1}\overline{f}_2^{0} \\ \vdots \\ [S_m]^{-1}\overline{f}_m^{0} \end{bmatrix}. \tag{12}$$

Thus, (9) is a Jacobi iterative algorithm. Let

$$D = \begin{bmatrix} [S_1] & & & \\ & [S_2] & & \\ & & \ddots & \\ & & & [S_m] \end{bmatrix} \tag{13}$$

and

$$L = \begin{bmatrix} 0 & & & & \\ [V_{1,2}] & 0 & & & \\ [V_{1,3}] & [V_{2,3}] & 0 & & \\ \cdots & \cdots & \cdots & \ddots & \\ [V_{1,m}] & [V_{2,m}] & \cdots & [V_{m-1,m}] & 0 \end{bmatrix} \tag{14}$$

$$U = \begin{bmatrix} 0 & [V_{2,1}] & [V_{3,1}] & \cdots & [V_{m,1}] \\ & 0 & [V_{3,2}] & \cdots & [V_{m,2}] \\ & & 0 & \cdots & \cdots \\ & & & \ddots & [V_{m,m-1}] \\ & & & & 0 \end{bmatrix}. \tag{15}$$

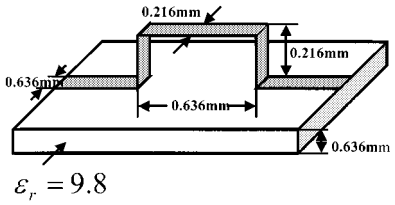

Fig. 4. Structure of the air-bridge.

Thus, (9) can be rewritten as

$$\overline{\Phi}^{(k+1)} = D^{-1}\left[(L+U)\overline{\Phi}^{(k)} + \mathbf{b}\right] \tag{16}$$

where

$$b = \begin{bmatrix} \overline{f}_1^0 \\ \overline{f}_2^0 \\ \vdots \\ \overline{f}_m^0 \end{bmatrix} \tag{17}$$

is the vector for all incident fields. Substituting the $(k+1)$th solution of the pth sub-domain ($p = \overline{1, i-1}$) into the computation of the $(k+1)$th solution of the ith sub-domain, the Gauss–Sediel iteration of (5) can then be obtained as follows:

$$\overline{\Phi}^{(k+1)} = D^{-1}\left(L\overline{\Phi}^{(k+1)} + U\overline{\Phi}^{(k)} + \mathbf{b}\right). \tag{18}$$

Compared with Jacobi iteration, it can save more memory and converges faster. Equation (18) can be rewritten as

$$\overline{\Phi}^{(k+1)} = G\overline{\Phi}^{(k)} + g \tag{19}$$

where

$$G = (D-L)^{-1}U \text{ and } g = (D-L)^{-1}\mathbf{b}.$$

III. Numerical Results

Fig. 4 shows a simple structure of the air-bridge that is often used in a multilayered printed circuit board (PCB). The whole domain is decomposed into three sub-domains along the transmission-line direction when the DDM is used (the decomposition is not presented in this figure). The S-parameters are plotted in Fig. 5 and we can find that the results calculated by the DDM agree very well with the data obtained by the FDTD method [15].

Fig. 6 shows the structure of a multilayered aperture-coupled patch antenna. The structure is decomposed into three and four sub-domains along the z-axis. The results of S_{11} are plotted in Fig. 7 and compared with published data [13]. Although the total number of unknowns is 685 506, just 7- and 54-MB RAM are the cost in the calculation, respectively. In this example, some fine adjustment of the patch antenna's parameters is made to satisfy the Yee-type FD lattice in the DDM–FD method, which results in a comparative big error , as shown in Fig. 7.

The new method can also be easily extended to the analysis of EM scattering by 3-D objects. Fig. 8 shows the magnitude and phase distribution of the z-direction current along path $\overline{abcd}$ on the surface of the conducting cube. In this example, the TM_z wave incidents along the $+x$-direction, and the side length s of the cube satisfies $k_0 s = 2.0$. The phase distribution in Fig. 8(b) takes the point a as the reference zero phase point. The results

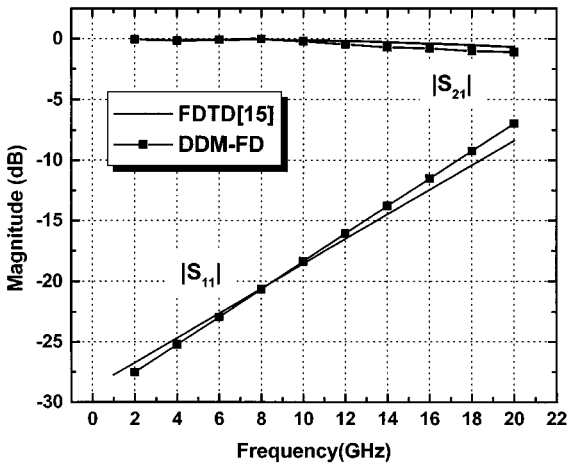

Fig. 5. S-parameters of the structure of the air-bridge shown in Fig. 4.

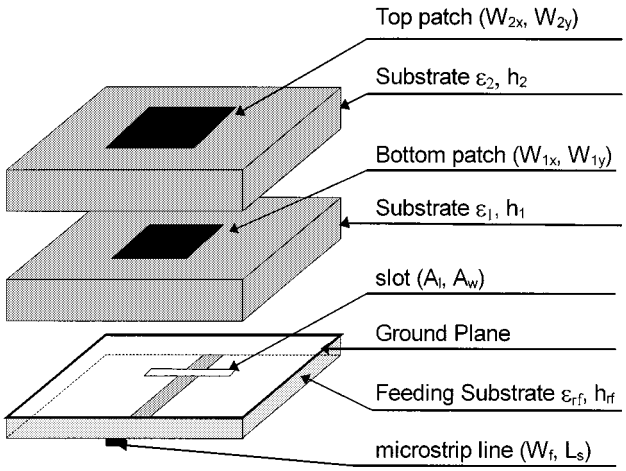

Fig. 6. Structure of the aperture-coupled stacked microstrip antenna $\varepsilon_2 = \varepsilon_1 = \varepsilon_{rf} = 2.2$, $W_{2x} = W_{2y} = 3.8$ mm, $W_{1x} = W_{1y} = 3.5$ mm, $A_l = 3.2$ mm, $A_w = 0.4$ mm, $W_f = 1.55$ mm, $L_s = 1.8$ mm, $h_2 = 1.0$ mm, $h_1 = h_{rf} = 0.5$ mm.

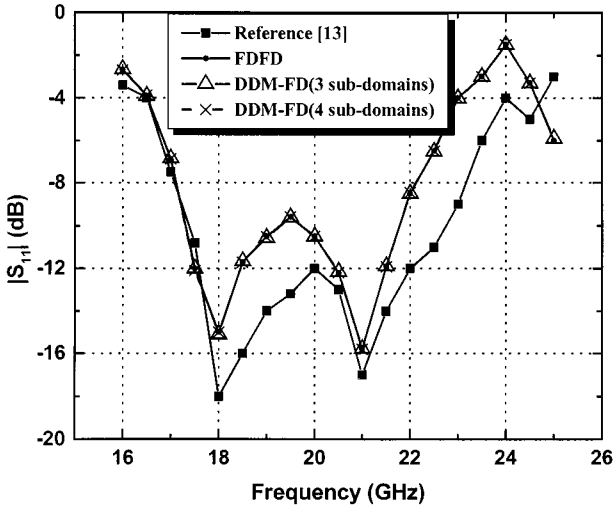

Fig. 7. S_{11} of the patch antenna shown in Fig. 6.

of this example are achieved on a PC PIII333/128MRAM. The memory and CPU time costs are listed in Table I when the number of sub-domains is different. Since the time for solving

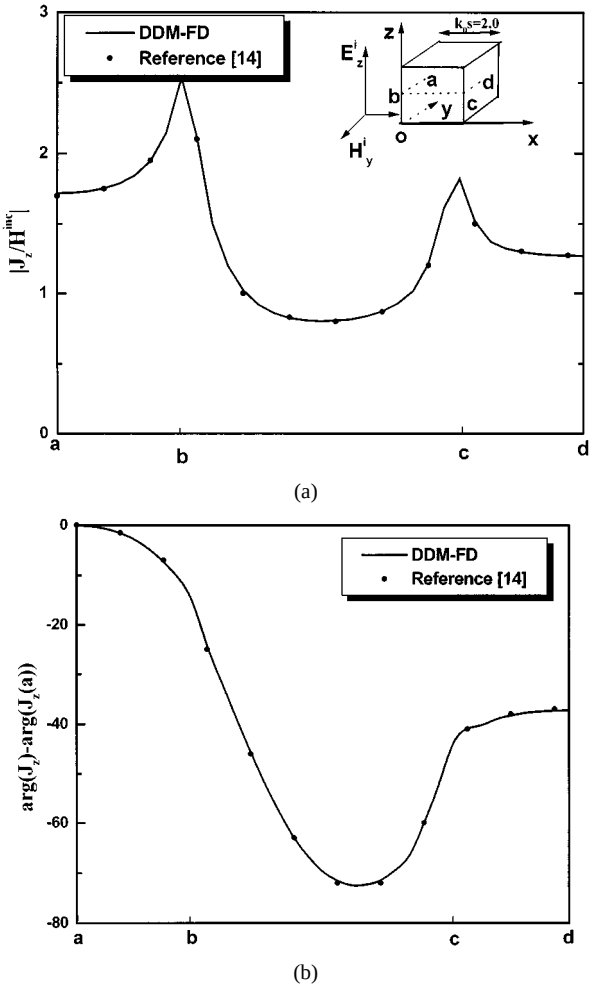

(a)

(b)

Fig. 8. (a) Magnitude of the z-direction current of path $\overline{abcd}$ on the surface of the conductive cube. (b) Phase of the z-direction current of path $\overline{abcd}$ on the surface of the conductive cube.

TABLE I
COMPARISON OF MEMORY AND CPU TIME WHEN THE NUMBER OF SUB-DOMAINS IS DIFFERENT (THE STRUCTURE IS SHOWN IN FIG. 8)

Number of sub-domains	Memory (MB)	Iteration steps	CPU time(s)
1	59.4	1	921
2	39.5	5	1325
3	23.2	6	1170

each sub-domain decreases when the number of sub-domains increases, the CPU time of the third case is shorter than that of the second case. Next, consider a conducting pillar with a rectangular cross section of size $k_0a \times k_0b = 2.0 \times 2.0$ and a finite length L in the z-direction. The corresponding bistatic radar cross sections (RCSs) from such three finite conducting pillars are shown in Fig. 9 for: (a) $k_0L = 2.0$; (b) $k_0L = 10.0$; and (c) $k_0L = 20.0$, respectively. The whole domain is divided into five sub-domains for each example.

IV. ACCELERATED ALGORITHMS

As mentioned above, by decomposing the whole 3-D structure into independent sub-domains, the DDM can greatly reduce the computational scale. However, we did not compare the computing time of the DDM with the conventional FDFD method because although it can save more memory, it cannot efficiently save CPU time in all cases. For example, for full-wave analysis of a 3-D structure, the FDFD method can be applied and then a sparse coefficient matrix with order N can be obtained, and then the computational effort of the FDFD method is proportional to ηN^2. Now, equally decompose the original domain into m sub-domains, and still employ the FDFD method to solve the EM equations in each sub-domain. The coefficient matrix $[S_i]$ corresponding to each sub-domain has the order of N/m. Since $[S_i]$ is still a sparse matrix, the computational effort of it is known as ξN^2. As we know, although the computational effort for solving a sparse matrix equation is cursorily proportional to N^2 in a general case, the actual computational effort will be increased with the enlargement of the matrix. Here, the constants η and ξ are used to express this variety. Hence, the total CPU time spent by the DDM–FD method can be estimated as

$$n \cdot m \cdot \xi O\left(\frac{N^2}{m^2}\right) = \frac{n}{m} \cdot \frac{\xi}{\eta} O\left(N^2\right)$$

where n is the total number of iteration steps. It is distinctive that the computational effort of the DDM–FD method is subjected to the coefficient $n/m \cdot \xi/\eta$. Unfortunately, the number of iteration steps n is often times larger than m, thus, the DDM–FD will cost more time in comparison with the FDFD method in most cases. From the above estimation, we can find that there are several ways to improve the computational efficiency of the new method as follows:

1) reduction of the iteration steps n;
2) faster solver for sub-domains;
3) parallel implementation.

Due to the restriction of the computer, parallel computation is hardly implemented for us. Thus, here we will try to enhance the computational efficiency of the DDM–FD method by reducing the iteration steps and finding a faster solver on each sub-domains. An irregular domain generally can be decomposed into some regular sub-domains; it then provides us the possibility of choosing the most efficient and even different faster solvers for different sub-domains. For some special sub-domains, even analytical solutions can be obtained.

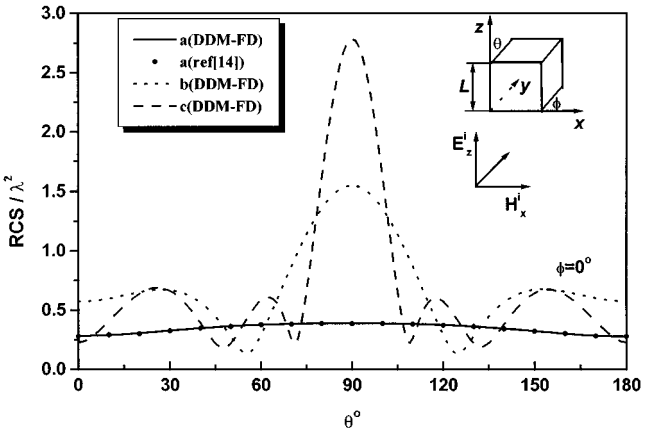

Fig. 9. RCS of the conductive pillar with a rectangular cross section of size $k_0a \times k_0b = 2.0 \times 2.0$ and a finite length L in the z-direction. (a)$k_0L = 2.0$. (b) $k_0L = 10.0$. (c) $k_0L = 20.0$.

TABLE II
COMPARISON BETWEEN THE RELAXATION FACTOR AND THE ITERATION STEPS (THE STRUCTURE IS SHOWN IN FIG. 4)

Number of sub-domains	Relaxation factor (w)	Iteration steps
2	0.1	32
	0.5	10
	0.7	9
	1.0	54
	1.5	73
3	0.1	40
	0.5	14
	0.7	12
	1.0	61
	1.5	83

A. Relaxation Iteration Algorithm

To reduce the iteration steps, we can use the following relaxation iterative equation instead of (18):

$$\overline{\Phi}_i^{(k+1)} = \overline{\Phi}_i^{(k)} + w[S_i]^{-1}\left[b_i + \sum_{j=1}^{i-1}[V_{j,i}]\overline{\Phi}_j^{(k+1)} - [S_i]\overline{\Phi}_i^{(k)} + \sum_{j=i+1}^{N}[V_{j,i}]\overline{\Phi}_j^{(k)}\right] \quad (20)$$

where w is the relaxation factor. The final relaxation algorithm can then be written as

$$\overline{\Phi}^{(k+1)} = S_w\overline{\Phi}^{(k)} + \boldsymbol{f} \quad (21)$$

where

$$S_w = (D - wL)^{-1}[(1-w)D + wU]$$
$$\boldsymbol{f} = w(D - wL)^{-1}\mathbf{b}$$

and w must satisfy the restriction $0 < w < 2$ to guarantee the convergence of the iterative procedure. Table II shows the relationship between the iteration steps and the relaxation factor when the DDM–FD method is used to analyze the patch antenna, shown in Fig. 6. From Table II, one can easily find that the relaxed algorithm shows better convergence performance. In this example, $w = 0.7$ is the best choice. Unfortunately, we cannot find the optimal w for different problems theoretically.

B. Overlapped Domain Decomposition

If the neighboring sub-domains are partially overlapped with each other, we then call the method an overlapped domain-decomposition method (ODDM). From both theoretical and physical concepts, we can conclude that the overlapped domain decomposition will results in a faster convergence rate because the information exchanged between conjunctional sub-domains is more plentiful. Although it is hard to theoretically analyze the relationship between the convergence rate and the overlapped proportion, one can intuitively conclude that the large overlapped area will bring a fast convergence rate. In fact, to overcome the drawback of a phase error, we have overlapped two conjoint sub-domains with half of the mesh space in our computation. Hence, the algorithm (5) can still be applied on overlapped domain decomposition. Table III listed the results of Fig. 4 calculated by overlapped domain decomposition. From Table III, one can find that the convergence rate of overlapped domain decomposition is nearly ten times faster than that of the nonoverlapped domain decomposition. In addition, it is also two times faster than relaxation iteration algorithm of nonoverlapped domain decomposition. Of course, the relaxation iteration algorithm can also be applied on the ODDM. If the whole domain is decomposed into two sub-domains, the number of overlapping layers is two and the relaxation is chosen to be 0.7, and the number of iteration steps will be reduced to five.

TABLE III
COMPARISON BETWEEN THE NUMBER OF OVERLAPPING LAYERS AND THE ITERATION STEPS (THE STRUCTURE IS SHOWN IN FIG. 4)

Number of sub-domains	Overlapping layers	Iteration steps
2	1	54
	2	17
	3	6
3	1	61
	2	20
	3	6

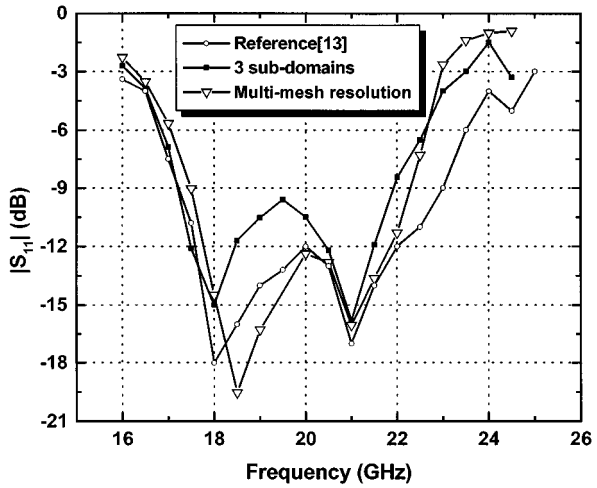

Fig. 10. S_{11} calculated by a multimesh resolution method and compared with a general DDM method.

C. Multimesh Resolution

Since some of the sub-domains may be very simple and regular, the same equidistance mesh for all the sub-domains is not economical in both memory and CPU time. Thus, localized quasi-uniformity grids can be used to discretize sub-domains, which means a different mesh resolution is adopted for different sub-domains. For convenience, the mesh spaces in sub-domains without discontinuity are double of those in sub-domains with discontinuity, and the meshes are chosen as Yee-type grids. The interpolation function

$$u(x, y) = a + bx + cy + dxy \quad (22)$$

is used to convert coarse mesh to fine mesh, and it can be rewritten in the FD format

$$u(x, y) = \sum_{i=1}^{4} u(x_i, y_i)\frac{(1 + x_i x)(1 + y_i y)}{4}, \qquad i = 1, 2, 3, 4. \quad (23)$$

Fig. 10 illustrates the results obtained by the above method. The improved DDM costs only half of the CPU time compared with the conventional global DDM.

V. Conclusion

In this paper, the DDM combined with the FDFD method has been presented for the full-wave analysis of 3-D EM problems. By using this method, we need not face the whole problem directly, but rather face some coupled sub-domains. Since these sub-domains can be divided in any possible form, it provides a possibility of applying a different efficient algorithm for a different sub-domain; e.g., even the analytic method can be used in a simple sub-domain for a complex problem. Examples, including the extraction of the S-parameters of an air-bridge structure, the analysis of patch antennas, and the scattering analysis of 3-D conductive pillars have been presented. All numerical results have demonstrated the validity of the new method. In Section IV, some accelerated algorithms have also been discussed to further improve computational efficiency.

Although the examples that have been presented in this paper are not very complex, they have still illustrated the advantages and flexibility of the method. Furthermore, this method is very suitable for parallel computation by using the Jacobi iterative procedure.

References

[1] T. Becks and I. Wolff, "Analysis of 3-D metallization structures by a full-wave spectral domain technique," *IEEE Trans. Microwave Theory Tech.*, vol. 40, pp. 2219–2227, Dec. 1992.

[2] R. Runger and F. Arndt, "Efficient MPIE approach for the analysis of three-dimensional microstrip structures in layered media," *IEEE Trans. Microwave Theory Tech.*, vol. 45, pp. 1141–1152, Aug. 1997.

[3] J. G. Yook, N. I. Dib, and L. P. B. Katehi, "Characterization of high frequency interconnects using finite difference time domain and finite-element methods," *IEEE Trans. Microwave Theory Tech.*, vol. 42, pp. 1727–1736, Sept. 1994.

[4] P. Mezzanotte, M. Mongriardo, L. Roselli, R. Sorrentino, and W. Heinrich, "Analysis of packaged microwave integrated circuits by FDTD," *IEEE Trans. Microwave Theory Tech.*, vol. 42, pp. 1796–1801, Sept. 1994.

[5] S. Haffa, D. Hollmann, and W. Wiesbeck, "The finite difference method for S-parameter calculation of arbitrary three-dimensional structures," *IEEE Trans. Microwave Theory Tech.*, vol. 40, pp. 1602–1609, Aug. 1992.

[6] Z. Bi, K. Wu, C. Wu, and J. Litva, "A dispersive boundary condition for microstrip component analysis using the FD-TD method," *IEEE Trans. Microwave Theory Tech.*, vol. 40, pp. 774–777, Apr. 1992.

[7] B. Desprès, "Domain decomposition method and the Helmholtz problem," in *Proc. Int. Math. Numer. Aspects Wave Propagat. Phenomena Symp.*, Strasbourg, France, 1992, pp. 44–52.

[8] ——, "A domain decomposition method for the harmonic Maxwell equations," in *Iterative Methods in Linear Algebra*. Amsterdam, The Netherlands: Elsevier, 1992, pp. 475–484.

[9] Z. H. Zhu, H. Ji, and W. Hong, "An efficient algorithm for the parameter extraction of 3-D interconnect structures in the VLSI circuits: Domain decomposition method," *IEEE Trans. Microwave Theory Tech.*, vol. 45, pp. 1179–1184, Aug. 1997.

[10] Z. H. Zhu and W. Hong, "A generalized algorithm for the capacitance extraction of 3-D VLSI interconnects," *IEEE Trans. Microwave Theory Tech.*, vol. 47, pp. 2027–2030, Oct. 1999.

[11] B. Strupfel, "A fast-domain decomposition method for the solution of electromagnetic scattering by large objects," *IEEE Trans. Antennas Propagat.*, vol. 44, pp. 1375–1385, Oct. 1996.

[12] L. Yin, X. Yin, and W. Hong, "A fast algorithm based on DDM and FMM for scattering by multi-cylinder," in *Proc. ISAPE'2000*, Beijing, China, p. 195.

[13] F. Croq and D. M. Pozar, "Millimeter-wave design of wide-band aperture-coupled stacked microstrip antennas," *IEEE Trans. Antennas Propagat.*, vol. 39, pp. 1770–1776, Dec. 1991.

[14] A. Taflove and K. Umashankar, "Radar cross section of general three-dimensional scatterers," *IEEE Trans. Electromagn. Compat.*, vol. EMC-25, pp. 433–440, Nov. 1983.

[15] M.-J. Tsai and C. Chen, *et al.*, "Multiple arbitrary shape via-hole and air-bridge transitions in multilayered structures," in *IEEE MTT-S Int. Microwave Symp. Dig.*, vol. 2, 1996, pp. 707–710.

Lei Yin was born in AnHui Province, China. He received the B.S., M.S., and Ph.D. degrees in radio science from Southeast University, Nanjing, China, in 1994, 1997, and 2000, respectively. His doctoral dissertation concerned the investigation of algorithms for full-wave analysis of 2-D and 3-D microwave components and structures.

He is currently a Software Engineer with Celestry Inc. San Jose, CA. From 1994 to 1995, he was with the State Key Laboratory of Millimeter Waves, Southeast University, where he was involved with research on microwave/millimeter-wave diplexer/multiplexer and filers. During this time, he wrote commercial software for design/analysis of waveguide filters.

Jie Wang was born in JiangSu Province, China. He received the B.S. and Ph.D. degrees in EM field and microwave techniques from the Southeast University of China, Nanjing, China, in 1996 and 2001, respectively.

His research interests include the DDM, matrix decomposition method, and parallel computation.

Wei Hong (M'92) was born in Hebei Province, China, on October 24, 1962. He received the B.S. degree from the Zhenzhou Institute of Technology, Zhenzhou, China, in 1982, and the M.S. and Ph.D. degrees from Southeast University, Nanjing, China, in 1985 and 1988, respectively, all in radio engineering.

Since 1988, he has been with the State Key Laboratory of Millimeter Waves, Southeast University, where he is currently a Professor and the Associate Dean of the Department of Radio Engineering. In 1993, 1995–1998, he was a short-term Visiting Scholar with the University of California at Berkeley and the University of California at Santa Cruz. He has authored and co-authored over 200 technical publications and also authored *Principle and Application of the Method of Lines* (Nanjing, China: Southeast Univ. Press, 1993). He served as a reviewer for many technical journals, including the *Proceedings of the Institution of Electrical Engineers, Part H, Electronics Letters*, etc. He has been engaged in numerical methods for EM problems, millimeter-wave theory and technology, antennas, EM scattering, inverse scattering and propagation, RF front-ends for mobile communications, the parameters extraction of interconnects in VLSI circuits, etc.

Prof. Hong is a senior member of the China Institute of Electronics (CIE). He served as the reviewer for many technical journals, including the IEEE Transactions on Microwave Theory and Techniques and the IEEE Transactions on Antennas and Propagaton. He was the two-time recipient of the first-class Science and Technology Progress Prizes presented by the State Education Commission in 1992 and 1994, respectively. He was the recipient of the 1991 Fourth-Class National Natural Science Prize and the Third-Class Science and Technology Progress Prize of Jiangsu Province. He was also the recipient of the Trans-Century Training Programme Foundation for the Talents presented by the State Education Commission, the Foundation for China Distinguished Young Investigators presented by the National Science Foundation (NSF), China, the Distinguished China Doctorate Recipients presented by the State Education Commission, and the JiangSu Young Scientist Award presented by the JiangSu Province Government.